

AMMAD ALI^{1,2}, JAE MIN SUNG^{1,3}, HYUN-WOO LEE^{1,3}, YOSEB SONG¹,
DA-WOON JEONG^{1,4}, KEE-RYUNG PARK^{1*}, BUM SUNG KIM^{1,2*}

ENCAPSULATION OF Ti POWDERS WITH WC-Co USING HIGH-ENERGY BALL MILLING: INFLUENCE OF MILLING TIME ON MICROSTRUCTURE

This work investigates the use of high-energy ball milling to encapsulate titanium (Ti) powders with tungsten carbide-cobalt (WC-Co). For varied amounts of time – between 1 and 12 hours – a combination of powders made up of 80% WC-Co and 20% Ti was milled. The findings show that WC was able to effectively encapsulate the surfaces of the Ti powders, and some of the Ti mechanically alloyed with Co to create an amorphous Co-Ti alloy. The encapsulation process is validated by microstructural analysis, which also shows how the powder shape changes during milling time. By providing a scalable approach for enhanced material synthesis, this encapsulation process has the potential to greatly improve the performance of Ti-based composites in wear-resistant applications and cutting tools.

Keywords: High-Energy Ball Milling; Ti Encapsulation; WC-Co Composites; Microstructure Evolution; Mechanical Alloying

1. Introduction

The pursuit of advanced materials for cutting tools and wear-resistant applications has been a significant focus of research for several decades. Cemented carbides, especially tungsten carbide-cobalt (WC-Co) composites, are renowned for their exceptional hardness, wear resistance, and toughness [1-4]. The cobalt (Co) binder in these composites enhances toughness and facilitates the sintering process [5-7]. However, the ongoing demand for improved material performance has driven research toward compositional modifications and structural optimization [8-13].

One approach that has drawn attention is the incorporation of titanium (Ti) into WC-Co composites. Ti is well known for its high strength-to-weight ratio, excellent corrosion resistance, and thermal stability. Previous studies suggest that Ti addition can potentially enhance toughness, oxidation resistance, and grain growth control during sintering, thereby contributing to improved high-temperature mechanical performance and structural uniformity in WC-Co-based systems [14-16]. However, these benefits are highly dependent on the dispersion, phase stability, and interfacial bonding of Ti within the composite matrix, which are significantly influenced by the powder prepara-

tion route [14-16]. Furthermore, Ti significantly improves the oxidation resistance of WC-Co composites, making them more suitable for high-temperature applications where oxidation can degrade material performance. The thermal stability imparted by Ti helps maintain the composite's mechanical properties at elevated temperatures, extending the service life of cutting tools and wear-resistant components [17]. Another critical advantage of Ti addition is its ability to inhibit grain growth during the sintering process. Fine-grained microstructures are known to enhance the hardness and wear resistance of composites, and Ti can act as a grain growth inhibitor, ensuring a more uniform and fine-grained structure [18,19]. This property is particularly valuable in maintaining the balance between hardness and toughness in WC-Co composites.

In this study, we focus on the synthesis and microstructural analysis of WC-Co-encapsulated Ti composite powders using high-energy ball milling [20,21]. The objective is to evaluate the encapsulation behavior of WC around Ti particles and to explore the formation of an amorphous Co-Ti phase during mechanical alloying [22]. A mixture containing 20% Ti and 80% WC-Co powders was milled for varying durations (1 to 12 hours) to analyze the evolution of morphology and phase characteristics.

¹ KOREA NATIONAL INSTITUTE OF RARE METALS, KOREA INSTITUTE OF INDUSTRIAL TECHNOLOGY, INCHEON, 21655, REPUBLIC OF KOREA

² UNIVERSITY OF SCIENCE AND TECHNOLOGY, INDUSTRIAL TECHNOLOGY AND SMART MANUFACTURING, DAEJEON, 34113, REPUBLIC OF KOREA

³ INHA UNIVERSITY, INCHEON, DEPARTMENT OF MATERIALS SCIENCE AND ENGINEERING, 22212, REPUBLIC OF KOREA

⁴ SCHOOL OF MECHANICAL ENGINEERING, CHUNG-ANG UNIVERSITY, SEOUL, REPUBLIC OF KOREA

* Corresponding authors: pkr86@kitech.re.kr; bskim15@kitech.re.kr



Microstructural analysis using X-ray diffraction (XRD) and scanning electron microscopy (SEM) was conducted to confirm the encapsulation process and understand the evolution of the powder morphology with milling time. The results indicate that WC successfully encapsulated the Ti powders' surfaces, and a portion of Ti mechanically alloyed with Co, forming an amorphous Co-Ti alloy. These findings suggest that the encapsulation technique can significantly enhance the performance of Ti-based composites.

The primary goal of this study is to demonstrate a scalable, efficient synthesis method for Co-Ti-containing composite powders with encapsulated morphology using high-energy ball milling. The microstructural evolution observed in this study may serve as a foundation for the development of next-generation WC-based materials, with enhanced performance to be evaluated in future work.

2. Experimental

2.1. Materials and Characterizations

WC-Co powders with average particle size of 28 μm and Ti powders with particle size of 1–20 μm were acquired from KRT corporation Korea. XRD analysis using a Bruker X-ray diffractometer and SEM combined with energy-dispersive X-ray spectroscopy (EDS) analysis using a JEOL equipment were two of the characterization techniques used.

2.2. Synthesis of WC-Co/Ti encapsulation

The synthesis of the encapsulated Ti and WC-Co composite powders was carried out using a high-energy ball milling machine. The milling process employed tungsten carbide (WC) jars and milling balls to ensure consistency and prevent contamination. A mixture comprising 20% Ti and 80% WC-Co powders was prepared and placed in the milling jars. The milling was conducted in an argon (Ar) environment to prevent oxidation of the powders during the process. The rotation speed was main-

tained at 300 rpm, with a ball-to-powder weight ratio of 10:1. To study the effect of milling time on the encapsulation and alloying process, samples were collected at regular intervals of 1 hour, 3 hours, 6 hours, 9 hours, and 12 hours. This systematic approach allowed for the analysis of the morphological and structural changes occurring at different stages of milling, providing insights into the optimal conditions for achieving uniform encapsulation and potential alloy formation.

3. Results and discussion

The SEM images illustrating the morphologies of the starting powders prior to composite synthesis are presented in Fig. 1. The WC-Co particles, shown in Fig. 1(a), are characterized by round, porous agglomerates, reflecting a composite structure of WC and Co. This morphology indicates a well-mixed, homogeneous distribution of the WC and Co phases within the initial WC-Co powder. In contrast, the Ti particles, shown in Fig. 1(b), have irregular shapes, indicating a non-uniform distribution of Ti within the starting Ti powder. These initial microstructural observations provide a basis for understanding the starting materials and guide the subsequent stages of composite synthesis and characterization.

Fig. 2 illustrates the XRD patterns of the initial powder mixture and the powders milled for different durations (1, 3, 6, 9, and 12 hours). The JCPDS reference numbers used for phase identification are WC (025-1047), Co (001-1255), and Ti (01-1197). The un-milled sample exhibits sharp and well-defined peaks at approximately 35.8°, 40.0°, 44.2°, and 63.0°, which can be attributed to the (100), (101), and (110) planes of Ti and Co, along with dominant peaks from the WC phase. These reflections confirm the crystalline nature and phase purity of the starting powders.

After 1 hour of milling, the XRD pattern still shows the presence of distinct Ti and Co peaks, although with slight intensity reduction and marginal peak broadening. This suggests partial fragmentation and early-stage alloying, but no significant structural transformation has yet occurred. The mechanical interaction during this stage is not sufficient to induce full amorphization or significant grain refinement.

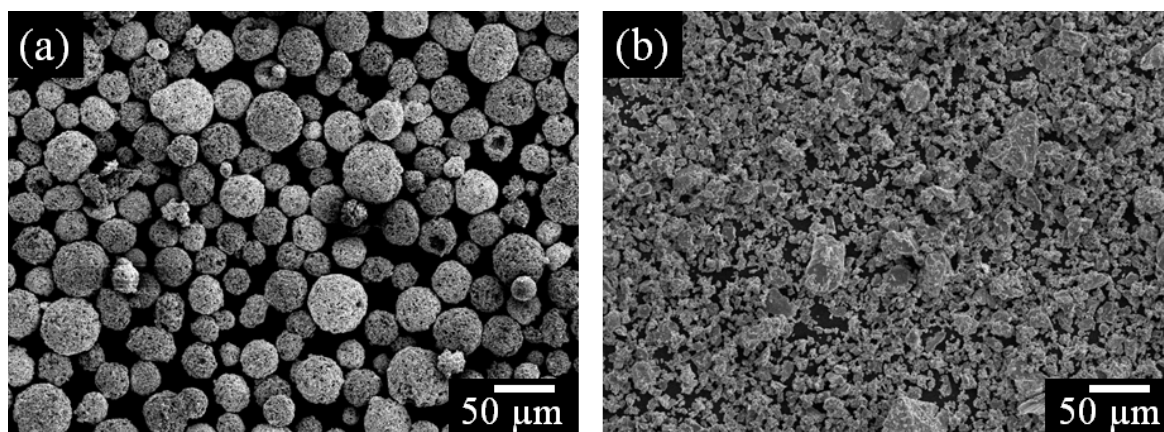


Fig. 1. (a) as received WC-Co powders, (b) as received Ti powders

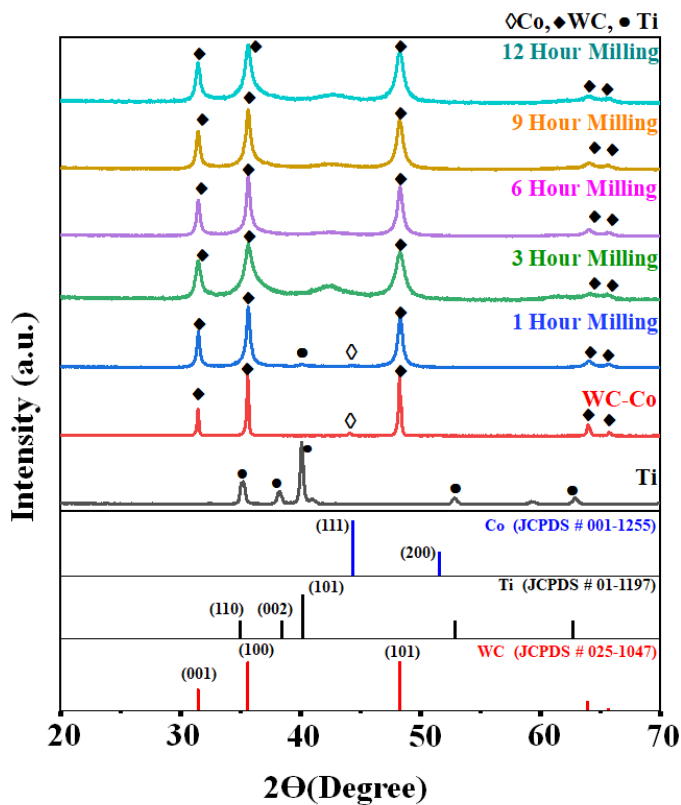


Fig. 2. XRD analysis of as received powders v/s the milled powders at various time intervals

By 3 hours of milling, a marked structural change is observed. The peaks corresponding to Ti (around 35.0°) and Co (around 44.2°) have disappeared or significantly diminished, indicating the dissolution of these elements into an amorphous

matrix. This disappearance is a classic signature of mechanical alloying, where repeated cold welding, fracturing, and rewelding lead to the formation of a Co-Ti amorphous phase [22]. The simultaneous peak broadening observed for WC (especially around 31.6° , 35.6° , and 48.4° , corresponding to the (001), (100), and (101) planes) implies either the onset of nano-crystallization or the development of lattice strain induced by high-energy impacts [23].

With further milling at 6, 9, and 12 hours, the WC peaks continue to broaden, and their intensity becomes more diffuse. This sustained broadening can be attributed to:

Progressive particle size reduction, as supported by SEM analysis, and Introduction of microstrain and crystal defects into the WC lattice due to mechanical deformation.

Notably, no new crystalline phases such as TiN or TiC appear in the XRD spectra, confirming that nitriding or carbothermal reactions have not occurred during milling. The Co-Ti amorphous structure appears to persist, as no crystalline intermetallics like CoTi or Co₂Ti are detected. These XRD results collectively confirm two key effects of mechanical milling: Successful alloying of Ti and Co into a non-crystalline Co-Ti phase, and Microstructural refinement of WC, likely enhancing the sinterability and potential mechanical performance of the composite powder in subsequent applications. Microstructural changes at different milling durations are shown in the SEM images of the polished cross-sections of the milled powders, as presented in Fig. 3. At 1 hour of milling, the SEM images show that the round agglomerates of WC-Co have begun to break apart, but full encapsulation of the Ti particles is not yet evident. The Ti particles remain relatively distinct with irregular shapes, while the WC-Co particles exhibit signs of disruption. By 3 hours, the Ti particles become more

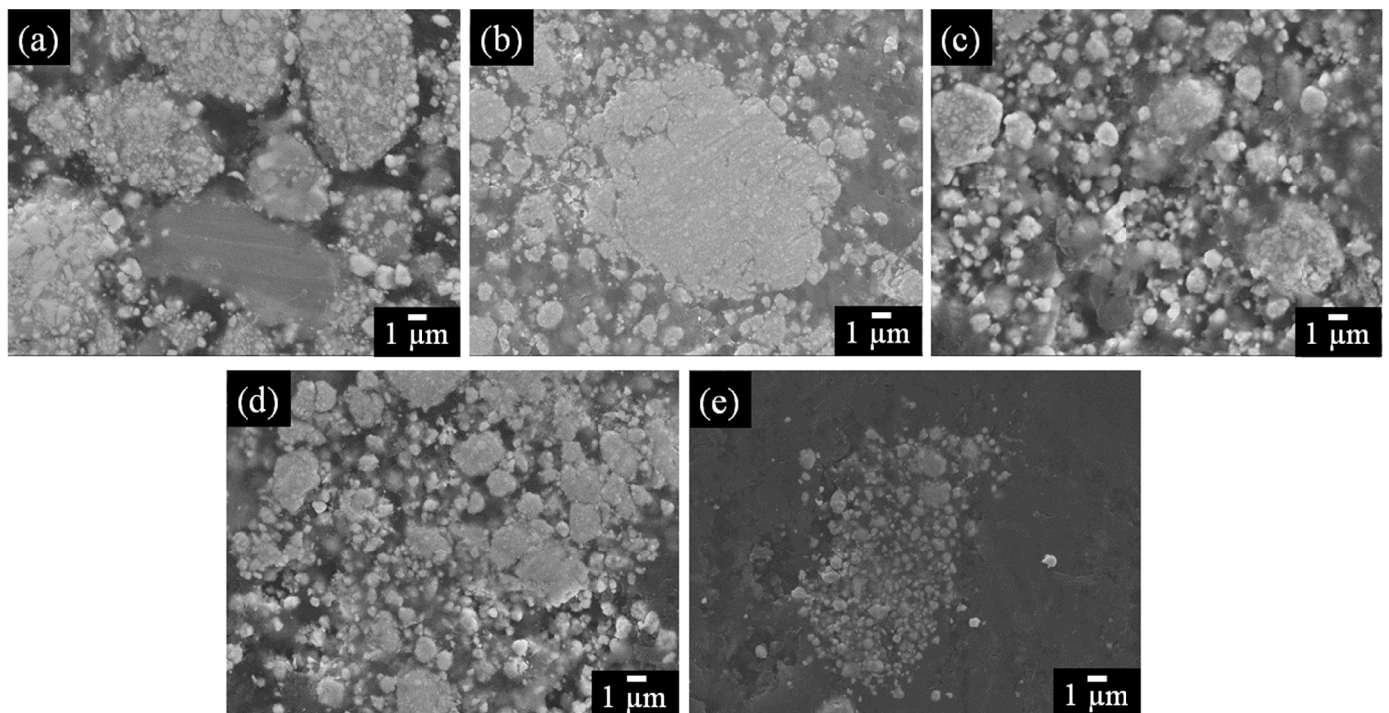


Fig. 3. SEM analysis, cross-section of WC-Co-Ti20 milled powders (a) 1 hour milling, (b) 3 hours milling, (c) 6 hours milling, (d) 9 hours Milling, (e) 12 hours milling

integrated within the WC-Co matrix, and the distinct separation between Ti and WC-Co begins to blur, reflecting early-stage encapsulation and the onset of amorphous phase formation.

At 6 and 9 hours, further milling causes cold welding, particle flattening, and agglomerate fragmentation. A significant portion of the Ti particles is enveloped within the WC-Co matrix. The distribution becomes more homogeneous, and the contrast between different phases fades, indicating increasing interface diffusion and the development of a core-shell-like morphology.

By 12 hours, the powder morphology appears highly refined and uniform, with submicron particles predominating. The WC-Co regions are no longer porous but appear densely compacted and well-dispersed around the Ti-rich domains. The amorphous phase formation, as supported by the disappearance of Ti and Co peaks in XRD and elemental blending in EDS, becomes more evident through the lack of sharp phase boundaries.

These SEM findings, when correlated with the XRD and EDS results, confirm the effectiveness of high-energy ball mill-

ing in transforming heterogeneous powders into a structurally integrated, nanostructured composite system. The improved homogeneity and fine particle morphology may contribute to better packing behavior and sinterability in future consolidation processes. As milling continues to 6, 9, and 12 hours, further refinement is observed. The particles become finer and more uniformly distributed throughout the matrix. The WC-Co particles, initially rounded and porous, are now more uniformly dispersed, and the particle size decreases, consistent with the broadening of WC peaks in the XRD patterns. Additionally, the amorphous phase becomes more prominent, with boundaries between different phases becoming less distinct. These SEM observations capture the progression from initial particle disruption to more homogeneous and refined composite structures due to extended milling

Fig. 4 presents SEM images and EDS elemental mapping of the powders after 1 hour of milling, capturing the earliest signs of microstructural and compositional transformation. The SEM

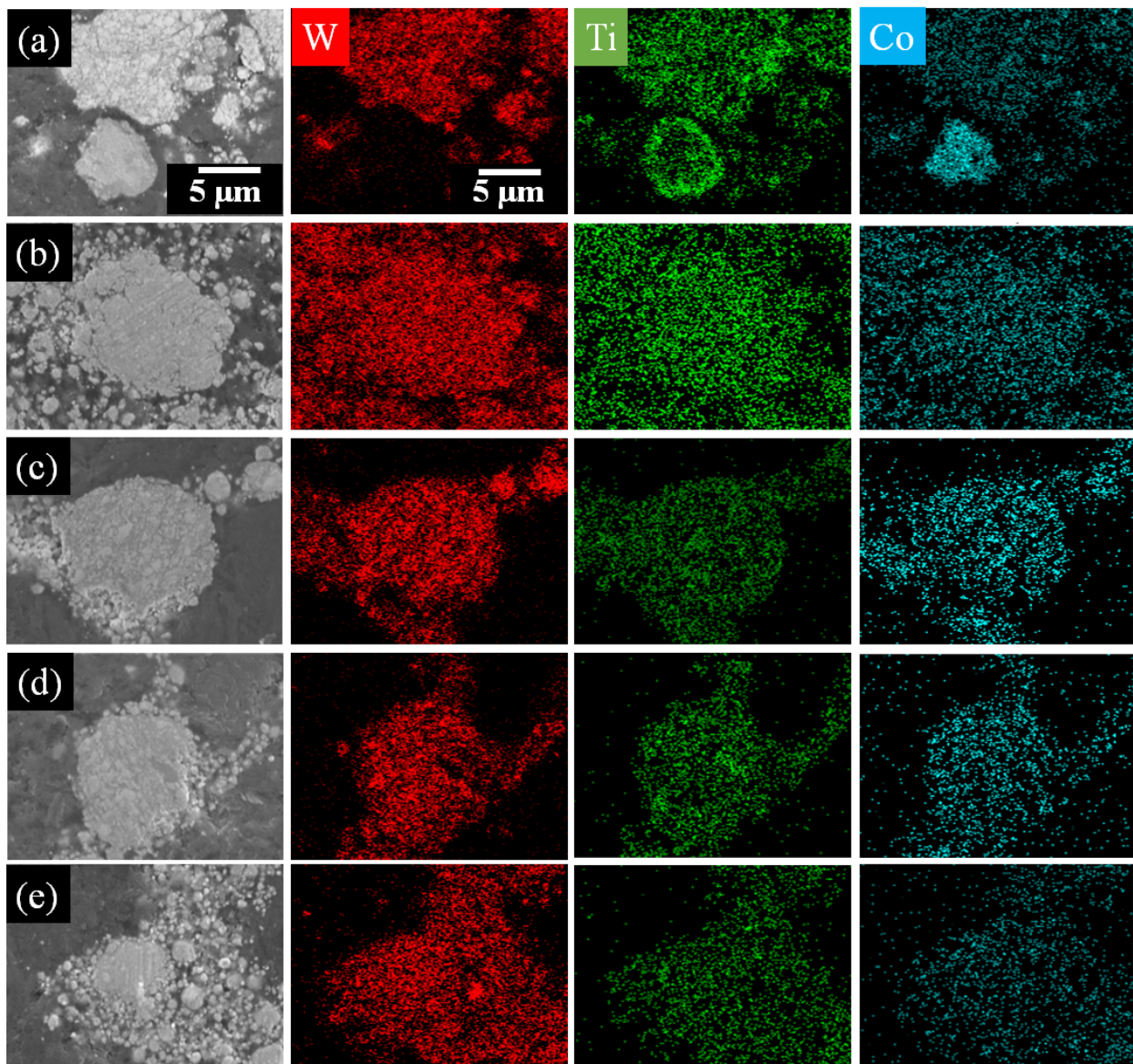


Fig. 4. SEM/EDS mapping of cross-section WC-Co-Ti20 milled powders (a) 1 hour milling, (b) 3 hours milling, (c) 6 hours milling, (d) 9 hours Milling, (e) 12 hours milling

image reveals that the WC-Co agglomerates are beginning to fracture under mechanical stress, with visible surface disruption and particle detachment. However, the Ti particles remain relatively intact and spatially distinct, indicating that encapsulation is still in its infancy. The corresponding EDS elemental maps offer deeper insight into phase distribution. W is primarily localized in dense, rounded agglomerates, while Ti appears in isolated zones with limited dispersion. Notably, the Co signal shows a transitional behavior: rather than remaining solely within the WC-Co domains, Co partially overlaps with adjacent Ti regions. This spatial merging suggests incipient mechanical alloying between Co and Ti. The overlap of Co and Ti signals, often visualized as blended or co-located colors in EDS maps (e.g., green and blue), implies the early development of a Co-Ti amorphous phase. This interpretation aligns well with the XRD data, which begins to show the weakening of Ti and Co peaks after just 1 hour of milling. The tendency of Co and Ti to form solid solutions or intermetallics under mechanical activation is well documented, and in this case, is driven by repeated cold welding and fracture mechanisms inherent to high-energy ball milling. Furthermore, the absence of significant W-Ti overlap confirms that WC does not react with Ti at this stage, but instead remains largely inert, supporting its role as an encapsulating agent. The initiation of Co-Ti bonding prior to full WC encapsulation underscores the sequential nature of the alloying process – with mechanical interdiffusion starting between the more ductile binder phase Co and Ti, and encapsulation progressing later as milling continues. These EDS observations, taken together with SEM and XRD data, confirm that even within 1 hour of processing, solid-state reactions and interfacial transformations are actively underway, setting the foundation for complete composite formation in later stages.

4. Conclusions

This research investigated the encapsulation of Ti powders within tungsten WC-Co matrices using high-energy ball milling. The study revealed that, at 1 hour of milling, the WC-Co particles began to break apart, and initial signs of mechanical alloying between Co and Ti were observed, resulting in the formation of a Co-Ti amorphous phase. As milling continued, the encapsulation of Ti by WC-Co became more pronounced, with XRD and SEM analyses indicating a transition towards a more homogeneous material. By 3 hours of milling, the distinct peaks of Ti and Co in the XRD patterns disappeared, reflecting the formation of an amorphous phase and partial encapsulation. Extended milling times of 6, 9, and 12 hours further refined the microstructure, resulting in finer particle sizes and more uniform distribution of the components, as evidenced by broadening WC peaks in the XRD patterns and consistent EDS mapping.

The addition of Ti demonstrated significant benefits, including improved toughness, oxidation resistance, and thermal stability of the WC-Co composites. The successful encapsulation and mechanical alloying observed in this study highlight the

potential of high-energy ball milling to enhance the performance of Ti-based composites. The findings suggest that this method can be effectively employed to develop advanced materials for cutting tools and wear-resistant applications, offering a scalable and efficient approach to material synthesis.

Acknowledgements

This work was supported by the project (PJE25160, 'Development of TiN hard surface treatment technology on powder for application of tungsten cemented carbide material in cooperation with NUST, Pakistan') funded by the Ministry of Economy and Finance (MOEF, Korea) as part of an international cooperation initiative

REFERENCES

- [1] S. Gaddam, S. Yadav, A.K. Behera, N. Arai, Z. Mahbooba, S.K. Jha, Q. Zhang, R.S. Mishra, Thermodynamics guided design and processing of a WC/HEA cermet tool for high temperature friction stir welding. *Mater. Des.* **250**, 113618 (2025). DOI: <https://doi.org/10.1016/j.matdes.2025.113618>
- [2] N.F. Lopes Dias, A.L. Meijer, C.P. Jäckel, A. Frisch, D. Biermann, W. Tillmann, Arc-enhanced glow discharge ion etching of WC-Co cemented carbide for improved PVD thin film adhesion and asymmetric cutting edge preparation of micro milling tools. *Surf. Coat. Technol.* **491**, 131166 (2024). DOI: <https://doi.org/10.1016/j.surfcoat.2024.131166>
- [3] H. Yamamoto, Y. Yamamoto, K. Ito, Y. Mikami, Compressive residual stress applied to a low-carbon steel surface alloyed with WC tool constituent elements according to friction stir processing. *Mater. Des.* **244**, 113225 (2024). DOI: <https://doi.org/10.1016/j.matdes.2024.113225>
- [4] B. Guimarães, C.M. Fernandes, D. Figueiredo, O. Carvalho, G. Miranda, F.S. Silva, Multi-material laser powder bed fusion of embedded thermocouples in WC-Co cutting tools. *J. Manuf. Process.* **118**, 163-172 (2024). DOI: <https://doi.org/10.1016/j.jmapro.2024.03.025>
- [5] K. Liu, Z. Wang, Z. Yin, L. Cao, J. Yuan, Effect of Co content on microstructure and mechanical properties of ultrafine grained WC-Co cemented carbide sintered by spark plasma sintering. *Ceram. Int.* **44**, 18711-18718 (2018). DOI: <https://doi.org/10.1016/j.ceramint.2018.07.100>
- [6] B. Wang, J. Jia, Z. Wang, Z. Yin, L. Huang, J. Yuan, Fabrication and performance of graded ultrafine WC-Co cemented carbide tool by one/two-step spark plasma sintering. *Ceram. Int.* **47**, 8322-8329 (2021). DOI: <https://doi.org/10.1016/j.ceramint.2020.11.194>
- [7] I. Konyashin, S. Hlawatschek, B. Ries, F. Lachmann, M. Vukovic, Cobalt capping on WC-Co hardmetals. Part I: A mechanism explaining the presence or absence of cobalt layers on hardmetal articles during sintering. *Int. J. Refract. Metals Hard Mater.* **42**, 142-150 (2014). DOI: <https://doi.org/10.1016/j.ijrmhm.2013.08.016>

- [8] G.H. Lee, S. Kang, Synthesis of nano-sized WC-Co powders by reduction-carburization process. *Mater. Trans.* **42**, 1575-1581 (2001). DOI: <https://doi.org/10.2320/matertrans.42.1575>
- [9] Q. Yang, J. Yang, H. Yang, H. Chen, W. Su, J. Ruan, Synthesis of ultrafine WC-Co composite powders under hydrogen atmosphere with in situ carbon via a one-step reduction-carbonization process. *Int. J. Appl. Ceram. Technol.* **14**, 220-227 (2017). DOI: <https://doi.org/10.1111/ijac.12628>
- [10] X. Wang, X. Song, X. Liu, X. Liu, H. Wang, C. Zhou, Orientation relationship in WC-Co composite nanoparticles synthesized by in situ reactions. *Nanotechnology* **26** (2015). DOI: <https://doi.org/10.1088/0957-4484/26/14/145705>
- [11] Y. Li, K. Xie, J. Ye, Z. Meng, L. Liao, Preparation of core-shell WC-Co composite powder. *Materials Research Innovations* **18**, 289-293 (2014). DOI: <https://doi.org/10.1179/1433075X13Y.0000000145>
- [12] Y. Wu, Z. Lu, Y. Qin, Z. Bao, L. Luo, Ultrafine/nano WC-Co cemented carbide: Overview of preparation and key technologies. *Journal of Materials Research and Technology* **27**, 5822-5839 (2023). DOI: <https://doi.org/10.1016/j.jmrt.2023.10.315>
- [13] Q. Yang, J. Yang, H. Yang, W. Su, J. Ruan, Synthesis and characterization of WC-Co nanosized composite powders with in situ carbon and gas carbon sources. *Metals and Materials International* **22**, 663-669 (2016). DOI: <https://doi.org/10.1007/S12540-016-6033-6>.
- [14] L. Heydari, P.F. Lictor, F.A. Corpas-Iglesias, O.H. Laguna, Ti(C,N) and WC-Based Cermets: A Review of Synthesis, Properties and Applications in Additive Manufacturing. *Materials* **14**, 6786 (2021). DOI: <https://doi.org/10.3390/ma14226786>
- [15] J. Tan, S. Wen, Y. Liu, Y. Du, G. Kaptay, Thermal conductivity of WC-Co-TiC cemented carbides: Measurement and modeling. *Int. J. Refract. Metals Hard Mater.* **112**, 106153 (2023). DOI: <https://doi.org/10.1016/j.ijrmhm.2023.106153>
- [16] D. Garbiec, A.M. Laptev, V. Leshchynsky, M. Wiśniewska, P. Figiel, A. Biedunkiewicz, P. Siwak, J. Räthel, J. Pötschke, M. Herrmann, Spark plasma sintering of WC-Ti powder mixtures and properties of obtained composites. *J. Eur. Ceram. Soc.* **42**, 2039-2047 (2022). DOI: <https://doi.org/10.1016/j.jeurceramsoc.2022.01.002>
- [17] J. Mikuła, D. Pakuła, L. Żukowska, K. Gołombek, A. Kříž, Wear Resistance of (Ti,Al)N Metallic Coatings for Extremal Working Conditions. *Coatings* **11**, 157 (2021). DOI: <https://doi.org/10.3390/coatings11020157>
- [18] X. Wang, J. Zhao, E. Cui, Z. Sun, H. Yu, Grain growth kinetics and grain refinement mechanism in Al₂O₃/WC/TiC/graphene ceramic composite. *J. Eur. Ceram. Soc.* **41**, 1391-1398 (2021). DOI: <https://doi.org/10.1016/j.jeurceramsoc.2020.10.019>
- [19] Z. Zhao, D. Li, X. Yan, Y. Chen, Z. Jia, D. Zhang, M. Han, X. Wang, G. Liu, X. Liu, S. Liu, Insights into the dual effects of Ti on the grain refinement and mechanical properties of hypoeutectic Al-Si alloys. *J. Mater. Sci. Technol.* **189**, 44-59 (2024). DOI: <https://doi.org/10.1016/j.jmst.2023.12.014>
- [20] C. Suryanarayana, Mechanical alloying and milling. *Prog. Mater. Sci.* **46**, 1-184 (2001). DOI: [https://doi.org/10.1016/S0079-6425\(99\)00010-9](https://doi.org/10.1016/S0079-6425(99)00010-9)
- [21] J.S. Benjamin, Mechanical alloying – A perspective. *Metal Powder Report* **45**, 122-127 (1990). DOI: [https://doi.org/10.1016/S0026-0657\(10\)80124-9](https://doi.org/10.1016/S0026-0657(10)80124-9)
- [22] R. Martínez-Sánchez, J.A. Matutes-Aquino, O. Ayala-Valenzuela, S.D. De La Torre, Magnetic properties of mechanically alloyed Co-Ti powder. *Physica B Condens Matter* **320**, 285-287 (2002). DOI: [https://doi.org/10.1016/S0921-4526\(02\)00716-0](https://doi.org/10.1016/S0921-4526(02)00716-0)
- [23] C.C. Koch, Optimization of strength and ductility in nanocrystalline and ultrafine grained metals. *Scr. Mater.* **49**, 657-662 (2003). DOI: [https://doi.org/10.1016/S1359-6462\(03\)00394-4](https://doi.org/10.1016/S1359-6462(03)00394-4)